

Scanning Electron Microscopy

Volume 1982
Number 1 1982

Article 7

1982

Gaussian Models for the Energy Distribution of Excitation in Solids: Applications to X-Ray Microanalysis and Solid State Electronics

David B. Wittry
University of Southern California

Follow this and additional works at: <https://digitalcommons.usu.edu/electron>



Part of the [Biology Commons](#)

Recommended Citation

Wittry, David B. (1982) "Gaussian Models for the Energy Distribution of Excitation in Solids: Applications to X-Ray Microanalysis and Solid State Electronics," *Scanning Electron Microscopy*. Vol. 1982 : No. 1 , Article 7.

Available at: <https://digitalcommons.usu.edu/electron/vol1982/iss1/7>

This Article is brought to you for free and open access by the Western Dairy Center at DigitalCommons@USU. It has been accepted for inclusion in Scanning Electron Microscopy by an authorized administrator of DigitalCommons@USU. For more information, please contact digitalcommons@usu.edu.



GAUSSIAN MODELS FOR THE ENERGY DISTRIBUTION OF EXCITATION IN SOLIDS: APPLICATIONS TO X-RAY MICROANALYSIS AND SOLID STATE ELECTRONICS*

DAVID B. WITTRY

Departments of Materials Science and Electrical Engineering
University of Southern California
Los Angeles, CA 90007
(213) 743-2510

ABSTRACT

Gaussian models for the depth distribution of excitation in a solid bombarded by an electron beam have been successfully applied to the interpretation of data obtained in electron probe x-ray microanalysis (spatial resolution and absorption effects) and to the study of voltage dependence of cathodoluminescence and the voltage dependence of electron beam induced currents at Schottky barriers. In these applications, it was assumed that the distribution of excitation with depth can be scaled in depth according to the range-energy equation: $R = CE_0^n$. The physical basis for this range-energy equation is the Bethe equation for electron energy loss, which yields the Bethe range when integrated over the electron's path in the target. The "Bethe" range was previously shown by Hoff and Everhart to be of the form $R = CE_0^n$ over the range of energies useful in most experiments with electron beam excitation.

Keywords and phrases: Gaussian models, range-energy equations, Bethe range, principle of scaling, x-ray absorption correction factor, x-ray absorption coefficients, resolution of electron probe x-ray microanalysis, cathodoluminescence, electron beam induced current.

INTRODUCTION

The spatial distribution of electron beam excitation in a solid target has been an important parameter for the interpretation of results from a wide variety of experiments involving electron bombardment; these include scanning electron microscopy, x-ray microanalysis, cathodoluminescence, electron beam induced currents, electron beam recording, and electron beam lithography. Some of the methods that have been used to obtain information on this vital quantity are: 1) tracer methods using characteristic x-rays, 2) luminescence of gases or of solids, 3) electron beam induced currents across thin buried SiO₂ layers, 4) exposure of electron resists, 5) transport model calculations and 6) Monte Carlo calculations. For purposes of calculation, several analytic approximations have been used for the spatial distribution of excitation. The most useful analytic functions for the depth distribution of excitation have been a shifted Gaussian (Wittry and Kyser, 1967), a cubic polynomial (Everhart and Hoff, 1971), a shifted Gaussian with an exponential function subtracted (Kyser, 1972) and a non-shifted Gaussian multiplying a term resembling a complementary exponential function (Packwood and Brown, 1980, 1981).

The basic idea of using a Gaussian function to describe the distribution of excitation with depth has its origin in some of the work published in 1953 by Castaing and Descamps. Castaing and Descamps (1953) chose to express the results of their tracer experiments on the depth distribution of excitation $\phi(qz)$ on a log-linear plot. The close resemblance of this plot to a parabolic function suggested that a shifted Gaussian would provide a good approximation to the distribution of excitation with depth. The agreement of theoretical calculations based on this approximation and the principle of scaling with experimental results for several types of experiment has shown that the Gaussian model is quite useful in practical applications. In this paper, several cases in which the Gaussian model has been useful will be reviewed.

GAUSSIAN MODELS

The Gaussian model for distribution of excitation with depth can be expressed in its simplest form as follows:

$$\phi(qz) = A_0 \exp \left[- \left(\frac{qz - qz_0}{q\Delta z} \right)^2 \right] \quad (1)$$

*This work was supported by the Air Force Office of Scientific Research. The United States Government is authorized to reproduce and distribute reprints for Government purposes notwithstanding any copyright notation hereon.

LIST OF SYMBOLS

A	= Atomic weight	η_q	= Quantum efficiency for bulk radiative recombination
A_0, A_1, A_2	= Constants in Gaussian approximations	Θ	= X-ray take off angle
a	= Constant in Bethe's law	Θ_s	= Scattering angle
b	= Constant in Kyser's approximation for $\phi(\rho z)$	μ	= X-ray linear absorption coefficient
C	= Constant in range energy equation	(μ/ρ)	= X-ray mass absorption coefficient ($\text{cm}^2 \text{gm}^{-1}$)
D_p	= Diffusion constant for holes (cm^2/sec)	π	= 3.14159...
d_p	= Thickness of dead layer (μm)	ρ	= Density (gm cm^{-3})
E	= Energy of an electron (keV)	σ_R	= Rutherford scattering cross section (cm^2)
E_0	= Energy of primary electrons (keV)	τ_p	= Lifetime of excess holes in n-type semiconductor
E_c	= Critical excitation energy (keV)	$\phi(\rho z)$	= Distribution of excitation with depth
e	= Charge on the electron	χ	= Argument of the absorption correction factor.
e_i	= Efficiency of electron beam induced current		
$f(\chi)$	= Absorption correction factor		
G_0	= Excess carrier generation rate ($\text{cm}^{-2} \text{sec}^{-1}$)		
I	= Mean ionization energy of atoms in a solid (keV)		
i	= Primary beam current (A)		
J_s	= Specimen current density (A cm^{-2})		
L	= Excess carrier diffusion length (μm)		
m	= Exponent in Kyser's Eq. for the generated intensity of characteristic lines		
N_A	= Avogadro's number		
n	= Exponent in range energy equation		
n_0	= Electron concentration in semiconductor		
p_0	= Hole concentration in semiconductor (cm^{-3})		
Δp	= Excess hole concentration in semiconductor (cm^{-3})		
q	= Constant in Brown's approximation to $\phi(\rho z)$		
R	= Range (μm)		
R_B	= Bethe range		
R_G	= Gruen range		
S	= Reduced surface recombination velocity		
s	= Surface recombination velocity (cm sec^{-1})		
u	= Depth in Schottky barrier specimen (cm)		
u_d	= Thickness of transition region for Schottky barrier (cm)		
u_m	= Thickness of metal region for Schottky barrier (cm)		
u_s	= Depth in semiconductor below transition region (cm)		
V_0	= Beam voltage (kV)		
\bar{V}	= Average energy of backscattered electrons (kV)		
w'	= Reduced electron range		
Z	= Atomic number		
z_0	= Depth of max. in Gaussian approximation (cm)		
z	= Depth in specimen (cm)		
Δz	= Standard deviation of Gaussian distribution of excitation with depth		
α	= Constant used by Packwood & Brown in $\phi(\rho z)$		
β	= Constant used by Packwood & Brown in $\phi(\rho z)$		
γ_0	= Constant used by Packwood & Brown in $\phi(\rho z)$		
ϵ	= Average energy to produce a hole-electron pair (eV)		
η	= Backscattering coefficient for electrons		
η_p	= Cathodoluminescence efficiency		

where z = depth from the surface, ρ = the target density and Δz determines the half-width of the Gaussian. This was used by Wittry and Kyser (1967). A modification of this function was suggested by Kyser (1972) to take account of the asymmetry of the distribution about the peak value. He suggested a function of the form:

$$\phi(\rho z) = A_1 \exp \left[- \left(\frac{\rho z - \rho z_0}{\rho \Delta z} \right)^2 \right] - A_2 \exp \left(- \frac{b \rho z}{\rho z_0} \right) \quad (2)$$

In practical applications of the functions given in Eq. 1 or Eq. 2, the constants are usually obtained by fitting experimentally determined $\phi(\rho z)$ curves or curves determined by Monte Carlo calculations (Bishop, 1965, 1967) or transport model calculations (Brown et al., 1969). Packwood and Brown (1980, 1981) chose to use a Gaussian function with a maximum at the surface with a multiplying term that would result in a slightly asymmetric Gaussian-like function, namely:

$$\phi(\rho z) = \gamma_0 \exp(-\alpha \rho z)^2 [(1 - q \exp(-\beta \rho z))] \quad (3)$$

Packwood and Brown have given expressions for the various constants ($\gamma_0, \alpha, q, \beta$) in Eq. 3 in terms of the atomic number Z , the incident beam voltage E_0 , the critical excitation potential E_c and the average energy for electron excitation I . Because of this more-detailed description of $\phi(\rho z)$, Packwood and Brown's function may provide a more accurate description of excitation in various targets with different primary beam energies and critical excitation voltages.

THE PRINCIPLE OF SCALING

In the interpretation of results of experiments using electron beam excitation it is usually necessary to know how the function $\phi(\rho z)$ or its Laplace transform varies with voltage. For example the Laplace transform of $\phi(\rho z)$ divided by integral of $\phi(\rho z)$ from zero to infinity is the absorption correction factor in quantitative electron probe microanalysis. Earlier work on the absorption correction factor indicated that it was possible to use a scaling factor related to the variation in the depth of the electron excitation based on a range-energy equation of the form:

Gaussian Models for Energy Distribution of Excitation

$$R = C E_0^n \quad (4)$$

where C is a constant, E_0 is the primary beam voltage (or energy) and n was an experimentally determined parameter.

The physical basis for this range-energy equation is the Bethe retardation law:

$$\frac{dE}{dx} = (2\pi N_A e^4) \left(\frac{Z}{A}\right) \frac{1}{E} \ln \frac{aE}{I} \quad (5)$$

where e is the charge on the electron, N_A is Avogadro's number, Z and A are the atomic number and atomic weight, a is a constant, and I is the mean ionization energy for electrons. The Bethe range may be defined by assuming a "continuous slowing down" approximation, namely:

$$R_B = \int_0^{E_0} \frac{dE}{dE/dx} = K \int_0^{\zeta(E_0)} \frac{d\zeta}{\zeta \ln \zeta} \quad (6)$$

where the constant $K = 9.4 \cdot 10^{-12} I^2 A/Z$ gm/cm³ if I is in eV and $\zeta = aE/I$. The result obtained by Everhart and Hoff is shown in Figure 1. For $a = 1.16$, aE/I would be 214.8, 107.4, and 34.2 for Al, Cu and Au respectively and $E_0 = 30$ keV. It can be seen that for a range of 3 to 30 keV the Bethe range is consistent with Eq. 4 with $n \approx 1.7$, a value frequently used and close to the value of 1.68 obtained by Andersen (1966) using x-ray measurements of SiO₂ layers on Si.

The principle of scaling is as follows: 1) it is assumed that $\phi(\rho z)$ remains of the same shape; 2) all values of $\phi(\rho z)$ are shifted along the z axis in proportion to the range as given by Eq. 4. The amplitude of $\phi(\rho z)$ is adjusted to correspond to the power dissipated in the specimen, namely $V_i(1 - \eta \bar{V}/V)$ where V and i are the voltage and current in the electron beam, η is the backscatter coefficient and \bar{V} is the average energy of the backscattered electrons. (Note, however, in some cases the backscatter correction is separated from the voltage dependence of $\phi(\rho z)$.) The fact that this principle of scaling is an approximation can be readily seen by comparison of Eq. 5 with the Rutherford scattering cross section:

$$\sigma_R \propto \left(\frac{Ze^2}{E}\right)^2 \frac{\sin^2 \theta}{\sin^4(\theta/2)} \quad (7)$$

where θ is the scattering angle. The voltage dependences of Eq. 5 and Eq. 7 are not the same, i.e., as the electron energy decreases, the scattering in a given distance of travel will increase more rapidly than the energy loss increases. Thus we expect the maximum of the $\phi(\rho z)$ curves to shift more toward the surface than would be predicted by simple scaling. This shift can be seen clearly in Figure 1 of Everhart and Hoff's paper (Everhart and Hoff, 1971). However, for a voltage range of a factor of 10, the shift is small and in most experiments the experimental errors are sufficiently large that this effect need not be considered.

APPLICATIONS TO X-RAY MICROANALYSIS

One of the earliest applications of a Gaussian approximation to X-ray microanalysis was the estimation of the volume excited by an infinitely small electron probe. Wittry (1958)

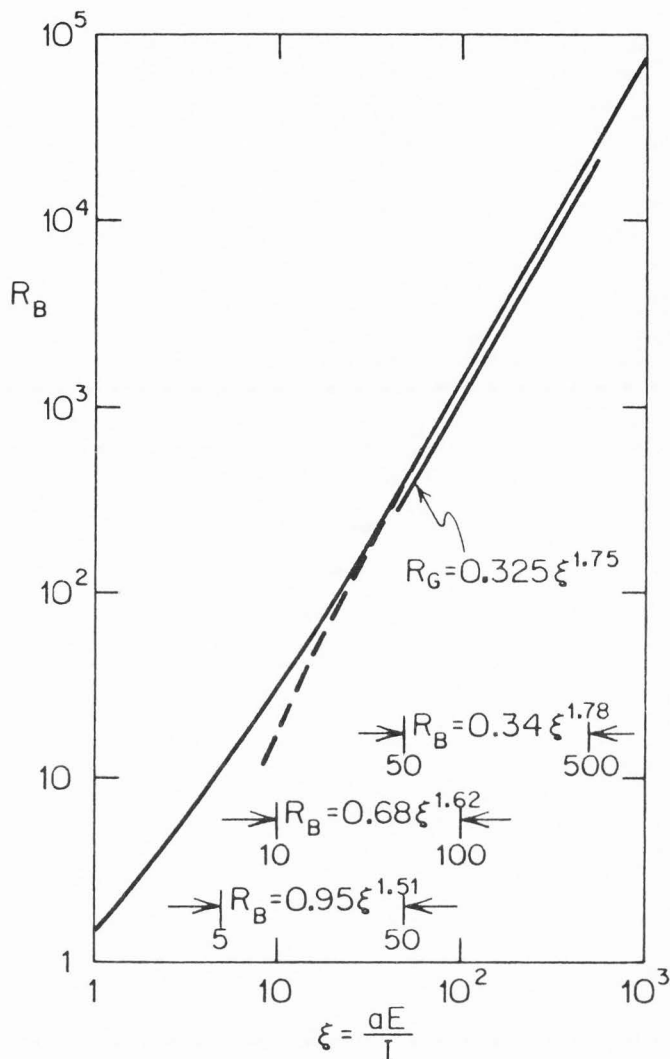


Fig. 1. Universal curve of normalized Bohr-Bethe range plotted vs. normalized electron energy. Normalization of both ordinate and abscissa depend on material atomic number, atomic weight, and constants only. Normalized range-energy relationships of the form $R_B = k \zeta^n$ accurate to a few percent are given for $5 < \zeta < 50$, $10 < \zeta < 100$, and $50 < \zeta < 500$. (This curve was calculated using a nonrelativistic formula.) (From Everhart and Hoff, 1971.)

assumed that the three-dimensional distribution was spherically symmetric about a point in the specimen corresponding to the maximum in the Gaussian approximation to $\phi(\rho z)$. Then, the depth distribution was used to deduce the three-dimensional excitation distribution. This was used to calculate the percent of excitation lying within a given spherical volume as shown in Figure 2. The three-dimensional spread of the excitation was also used to determine the optimum probe radius and voltage for best resolution and to determine the resolution that can be achieved when these quantities are optimized. In this case, the curves were scaled using an exponent $n = 1.7$ based on integration of Webster's form of Williams' retardation law.

Another important area for application of the Gaussian model has been in understanding the absorption correction factor in electron probe microanalysis. This is given by:

$$f(\chi) = \frac{\int_0^\infty \phi(\rho z) [\exp(-\chi \rho z)] d\rho z}{\int_0^\infty \phi(\rho z) d\rho z} \quad (8)$$

where $\chi = (\mu/\rho) \text{ cosec } \Theta$ and μ/ρ is the mass absorption coefficient. For the purpose of comparing various experimental determinations of $f(\chi)$ Andersen and Wittry (1968) devised a special scale for $f(\chi)$ that would yield straight lines when plotting $f(\chi)$ vs χ times the mean depth of x-ray production if $\phi(\rho z)$ is a Gaussian. This is shown in Figure 3. The mean depth of x-ray production was based on the Bethe x-ray range modified by a factor of $Z^{-1/3}$ (the Bethe range is obtained from Eq. 6 replacing $E = 0$ by $E = E_c$, the critical excitation potential). The fact that the data points lie close to a straight line verify the Gaussian nature of $\phi(\rho z)$ for a variety of experimental conditions.

The split of the data for $f(\chi) < .5$ is undoubtedly due to the excess x-ray generation predicted by the simple Gaussian model for $z < z_0$ and the large values of χ . As an example, Figure 4 shows a case where the simple Gaussian model would fail to give good results for large χ . In cases like this better results can be obtained with the lower curve in Figure 3.

One of the important aspects of the Gaussian model is that, combined with scaling, it can provide information concerning the voltage dependence of the x-ray absorption correction factor. Figure 5 shows a comparison of the observed voltage dependence of $\text{CK}\alpha$ x-rays from diamond as a function of the accelerating voltage. In this case, the conventional correction procedures gave very poor agreement with experimental results while the absorption correction of Figure 3 (lower curve) gave better results. Kyser (1972) used a modified Gaussian (Eq. 2) to evaluate $f(\chi)$ for $\text{FeL}_{\alpha 1,2}$ in Fe and showed that it provided good agreement with the lower $f(\chi)$ curve as shown in Figure 6.

Because of the ability to predict absorption correction factors vs voltage, it has been possible to determine absorption coefficients from experimental data on the voltage dependence of x-ray line intensities. This has proved to be a powerful tool particularly for soft x-ray lines for which conventional procedures have poor accuracy because of the extremely thin films that would be required. Kyser (1972) has evaluated mass absorption coefficients for $\text{L}\alpha_{1,2}$ lines from Ti, Cr, Mn, Fe, Co, Ni, Cu and Zn using data on the x-ray intensities vs. voltage. Typical data are shown in Figure 7. The mass absorption coefficients are obtained from the maximum intensity in the following equation:*

$$I_{\text{obs}} \propto E_0^m f(\chi, E_0) \quad (9)$$

The peak intensity depends on μ/ρ , n and m so that if n is taken to be 1.68, it is necessary to evaluate m in order to

*Kyser used n for the exponent in the intensity generation term and m for the exponent in the range energy equation. Because most authors use n in the range energy relation we have changed the notation from that used by Kyser.

determine χ . The constant m is evaluated by correcting the observed intensities for absorption to get the generated intensities, for example as shown in Figure 8. For the soft x-rays investigated, $\text{Ti L}\alpha$ through $\text{Zn L}\alpha$, and also for $\text{CK}\alpha$ it was found that $m \approx 1.2$ for $E_0 \gg E_c$ and μ/ρ ranged from 1,590 to 5,550 cm^2/gm .

On the basis of Kyser's (1972) work, Kyser and MacQueen (1972) proposed a new absorption correction function for soft x-rays based on a "truncated" Gaussian distribution. In recent years, Brown and his collaborators (Brown and Parobek, 1978, Brown and Robinson, 1979, Brown et al., 1969, and Packwood and Brown, 1980) have been evaluating correction factors for electron probe microanalysis using a somewhat different form of Gaussian expression for $\phi(\rho z)$. Their model for $\phi(\rho z)$ given in Eq. 3 has been used for relating intensities to mass concentrations directly in the absence of fluorescence corrections (Brown and Parobek, 1978, Brown and Robinson, 1979). This work is described in greater detail in another paper in this publication (p. 137).

APPLICATIONS TO SOLID STATE ELECTRONICS

For interpretation of results of experiments involving electron bombardment of semiconductors, it is important to know the distribution of excitation with depth. This can be utilized to obtain information on devices, such as the depth of p-n junctions, the thickness of metal layers, the electron beam current densities required to obtain stimulated emission, absorption of light emitted, etc. A knowledge of the voltage dependence of the excess carrier distribution can also be used to determine the diffusion length of excess carriers when the diffusion length is very small using the voltage dependence of cathodoluminescence or electron beam induced current (EBIC).

Using a Gaussian approximation to the energy dissipation function it is possible to solve the one-dimensional diffusion equation:

$$D_p \frac{d^2 \Delta p}{dz^2} - \frac{\Delta p}{\tau p} + C\phi(\rho z) = 0 \quad (10)$$

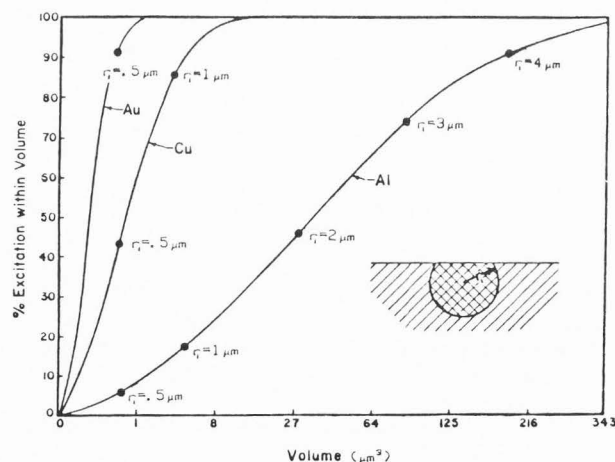


Fig. 2. Percent of excitation that is produced in a given volume based on a three-dimensional Gaussian distribution (from Wittry, 1958).

Gaussian Models for Energy Distribution of Excitation

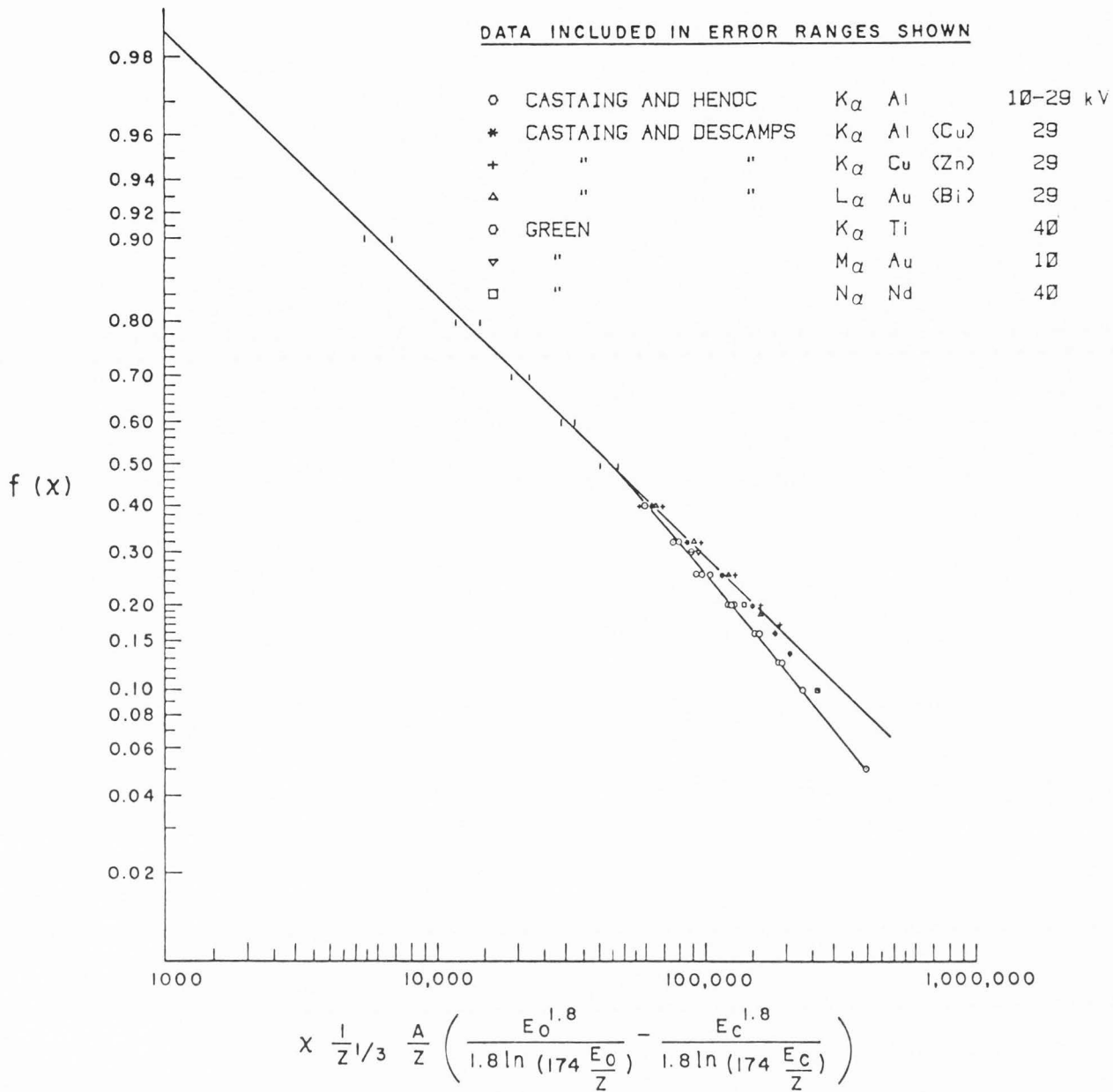


Fig. 3. Experimental data on the absorption correction function, $f(x)$ (from Andersen and Wittry, 1968).
© The Institute of Physics.

subject to the boundary condition:

$$D_p \frac{d\Delta p}{dz} \Big|_{z=0} = s\Delta p(0) \quad (11)$$

Here $\Delta p(z)$ is the excess carrier density, D_p the diffusion constant, τ_p the lifetime, L the diffusion length $= (D_p\tau_p)^{1/2}$, s is the surface recombination velocity and C is a constant relating the excess carrier generation function (carriers/cm²sec) to $\phi(\rho z)$. Similar equations would apply for electrons in p-type material. The constant C can be obtained by requiring that

$$C \int_0^\infty \phi(\rho z) dz = G_0 (\text{cm}^{-2}\text{sec}^{-1}) \quad (12)$$

where

$$G_0 = 6.25 \cdot 10^{21} \frac{V_0}{\epsilon} (1 - \eta \frac{\bar{V}}{V_0}) \frac{J_s}{1 - \eta} \quad (13)$$

where V_0 is the beam voltage in kV, J_s is the specimen current density in A/cm², \bar{V} the average energy of the backscattered electrons in kV, η is the fraction of incident electrons back-

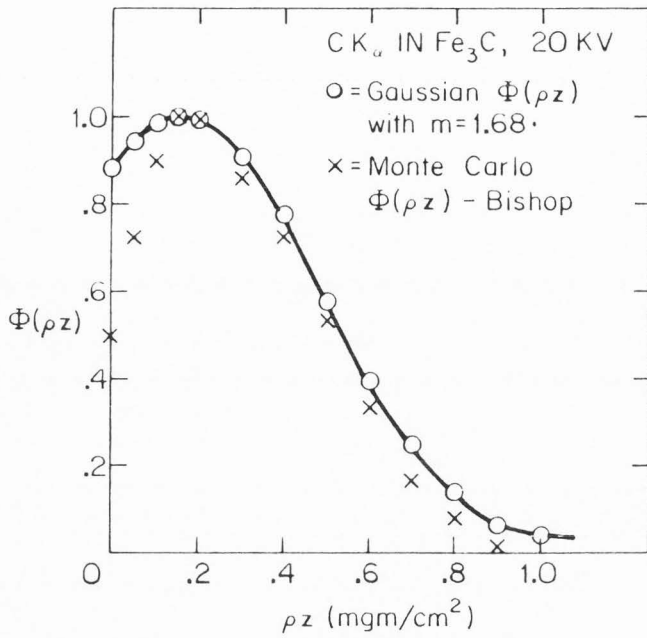


Fig. 4. Comparison of $\phi(\rho z)$ for CK_α in Fe₃C (from Kyser, 1972). (By permission of University of Tokyo Press).

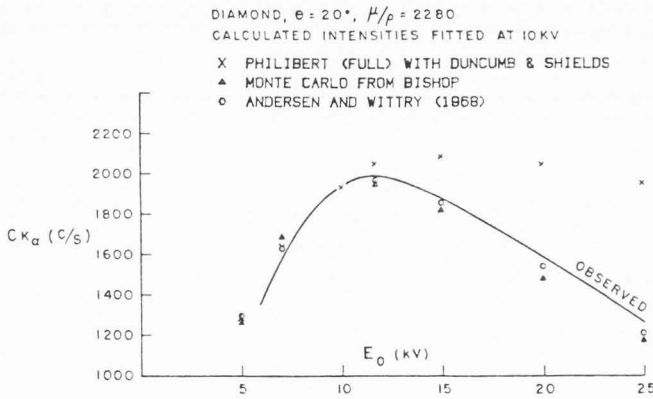


Fig. 5. Voltage dependence of x-ray intensities of carbon from diamond (from Andersen and Wittry, 1968). © The Institute of Physics.

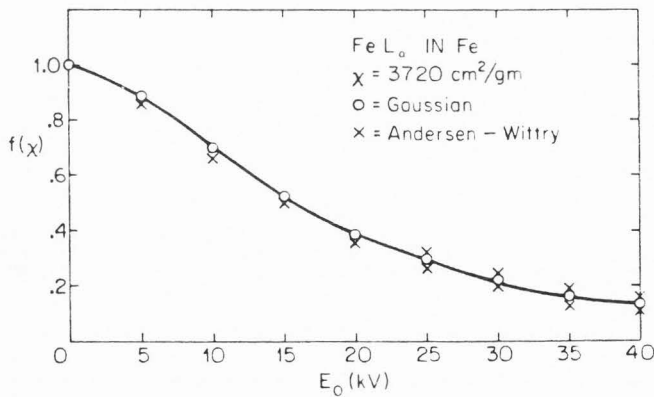


Fig. 6. Comparison of $f(\chi)$ for FeL_{α,1,2} in Fe (from Kyser, 1972). (By permission of University of Tokyo Press).

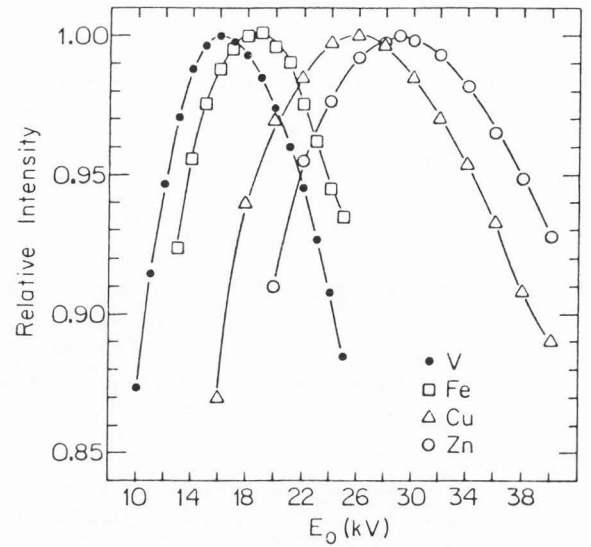


Fig. 7. Observed intensity vs. voltage for V, Fe, Cu, and Zn L_{α,1,2} in V, Fe, Cu, and Zn, respectively. The plotted data was digitally smoothed (from Kyser, 1972). (By permission of University of Tokyo Press).

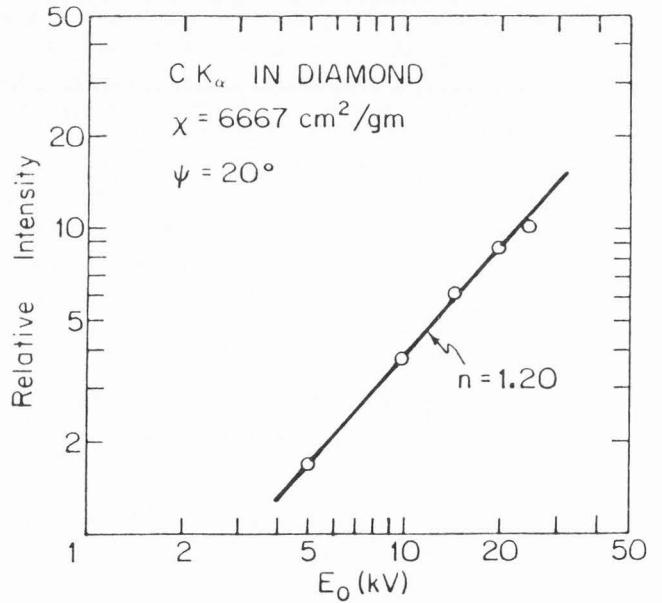


Fig. 8. Generated intensity vs. voltage for CK_α from diamond after an absorption correction was made to the data of Fig. 5 using the absorption correction of Fig. 3 (from Kyser, 1972). (By permission of University of Tokyo Press).

scattered and ϵ is the energy in electron volts required to create a hole-electron pair ($V/V_0 \cong 0.66$ and $\eta = 0.33$ for GaAs at 29 kV). An analytic solution is possible for equations 10 and 11 and the result is plotted in Figure 9.

The problem of predicting the voltage dependence of

Gaussian Models for Energy Distribution of Excitation

Fig. 9. Distribution in depth of carrier generation rate and carrier density for a 29 kV electron beam on GaAs. The left scale applies to the dotted line (Gaussian function) and to the open circles (transport model calculations). The right scale applies to the full lines for three values of reduced surface recombination velocity S . Parameter values used are $a^{1/2} = 0.66 \mu\text{m}^{-1}$, $z_0 = 0.65 \mu\text{m}$, $L = 0.76 \mu\text{m}$, $D_p = 3 \text{cm}^2 \text{sec}^{-1}$, $J = 2 \text{A/cm}^2$, and $\epsilon = 5.35 \text{eV}$ (from Kyser and Wittry, 1967). © 1967 IEEE.

Fig. 10. Calculated cathodoluminescence intensity as a function of the reduced electron range $w' = R/\rho L$ with $R = CE_0^n$ for various values of the reduced surface recombination velocity $S = (\text{surface recombination velocity})/(\text{diffusion velocity})$ assuming no "dead" layer. Voltage scales for an exponent n of 1.5 and 1.7 are shown. The plot applies for a diffusion length L of $1 \mu\text{m}$ and a voltage of 30 keV. The value of the diffusion length L can be obtained by translating experimental curves of $I(V)$ along the horizontal axis (from Wittry and Kyser, 1967).

cathodoluminescence intensities is only slightly more difficult. The basic assumption usually made is that the surface recombination is either non-radiative or the radiation produced is not detected. Therefore, one could first solve the diffusion equation and then evaluate the carrier loss due to surface recombination by determining the flux normal to the surface ($Dd\Delta p/dz$). Alternatively the boundary condition Eq. 11 could be replaced by a series of appropriately distributed sources and sinks and the flux due to these at the plane $z = 0$ could be calculated (Wittry and Kyser, 1967b). The result for the efficiency of cathodoluminescence η_p compared to the quantum efficiency η_q of the bulk can be expressed simply in terms of the Laplace transform of $\phi(\rho z)$, namely:

$$\frac{\eta_p}{\eta_q} = 1 - \frac{S}{S+1} \frac{\int_0^\infty \phi(\rho z) e^{-z/L} dz}{\int_0^\infty \phi(\rho z) dz} \quad (14)$$

where S is the reduced surface recombination $= \frac{\tau_p S}{L}$. Using

the principle of scaling, this equation can be used to predict the voltage dependence of cathodoluminescence.

However, experimental results obtained on GaAs show a much more rapid decrease in cathodoluminescence efficiency as the voltage is reduced than would be predicted by Eq. 14 and the principle of scaling. This may be explained if it is assumed that there is a "dead layer" at the surface due to band bending. In the band bending region, the excess minority carriers would drift rapidly to the surface and hence would not be able to participate in bulk radiative recombination. This case can be treated simply by assuming that the surface recombination occurs at a depth d (the thickness of the dead layer) from the surface. Typical results as a function of reduced electron range ($R/\rho L$) are shown in Figures 10 and 11 for $d/L = 0$ and $d/L = 0.05$. By using several families of

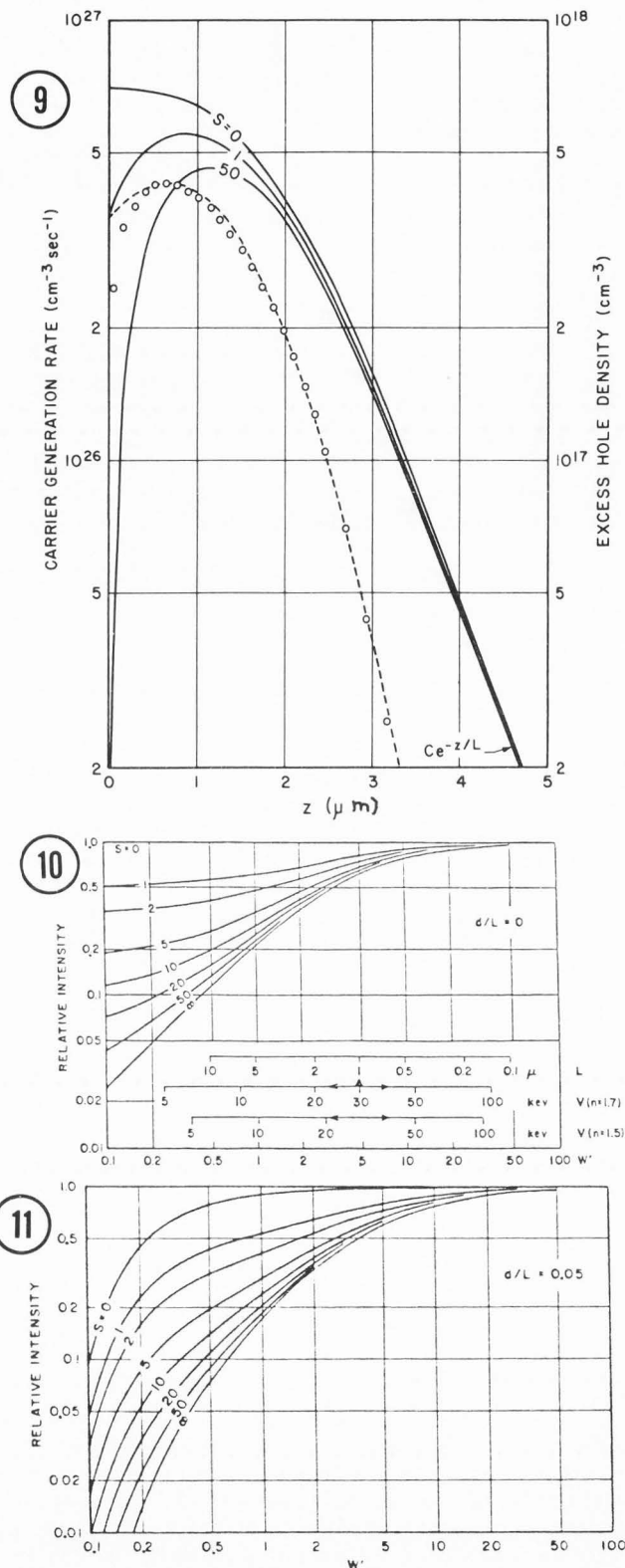


Fig. 11. Theoretical cathodoluminescence intensity as a function of the reduced electron range w' for various values of the reduced surface recombination velocity S for a "dead layer" of thickness $d = 0.05L$ (from Wittry and Kyser, 1967).

curves for various d/L , it is possible to fit experimental data quite well as shown in Figure 12 for n type GaAs. The fit of experimental data to theory leads to some ambiguity in determining S and d/L but various choices of these parameters give nearly the same values of diffusion length L in a given specimen. The values of S are typically ~ 20 or 50 , while d/L is $0.2-0.5$ for data shown in Figure 12. Independent knowledge of d would provide better values of S . Diffusion lengths for specimens 1-4 range from $0.65 \mu\text{m}$ for $n_0 = 3 \cdot 10^{18}$ to $3 \mu\text{m}$ for $n_0 = 5.1 \cdot 10^{16}$.

A study of the voltage dependence of cathodoluminescence in p -type material has also been made (Rao Sahib and Wittry 1969). However this experiment was complicated by a non-linear dependence of luminescence intensity on excess carrier density and it was necessary to include this in a phenomenological treatment to explain the observed results.

In a similar manner to voltage dependence of cathodoluminescence, a Gaussian model can be applied to currents induced at Schottky barriers by electron bombardment. In this case, however, the signal is analogous to what would correspond to the loss of signal in cathodoluminescence—namely the flux of carriers that arrive at a surface (in this case the metal-semiconductor interface). The model used, shown in Figure 13, divides the specimen into three regions. It is assumed that in the metal layer no carriers are produced, in the depletion layer all carriers produced are collected and in the bulk region carriers diffuse to the boundary of the depletion layer where they then drift rapidly across this layer. The calculation is similar to the calculation for cathodoluminescence. However in this case the boundary condition assumed is:

$$\Delta p(u_d) = 0 \quad (15)$$

The flux of carriers at u_d is calculated from $Dd\Delta p/dz$. The electron beam induced current is then the sum of the current due to carriers generated in the depletion layer and the current due to carriers diffusing to the boundary of the depletion layer. Typical theoretical curves are shown in Figure 14 and typical results for GaAs are shown in Figure 15. For comparing theory and experiment, the width of the depletion layer was estimated from published values of the surface barriers for the metal-semiconductor combinations used and the carrier concentrations. In Figure 15 the specimen with $L = 12 \mu\text{m}$ was epitaxially grown with $n_0 = 6.8 \cdot 10^{15}$, the specimen with $L = 0.64 \mu\text{m}$ was Czochralski grown with $n_0 = 1.3 \cdot 10^{15}$ and the specimen with $L = 0.41 \mu\text{m}$ was Czochralski grown with $n_0 = 1.1 \cdot 10^{18}$. Gold metallization was used for all 3 specimens with $u_m = 100 \mu\text{m}$ and $250 \mu\text{m}$.

The EBIC measurement provides accurate values for the metal layer thickness u_m and for L because the results are very sensitive to u_m at small voltage and to L at large voltage. Moreover, this experiment, in contrast to the cathodoluminescence experiment, provides quantitative results that can be compared to theory. As a result, it is possible to obtain a value for the average energy for creating a hole-electron pair by energetic electrons (this energy should not be voltage dependent for electrons with energy \gg the energy band gap). In this work, it was found that $\epsilon = 4.68 \pm 0.14 \text{ eV}$ in GaAs and $3.75 \pm 0.11 \text{ eV}$ in Si.

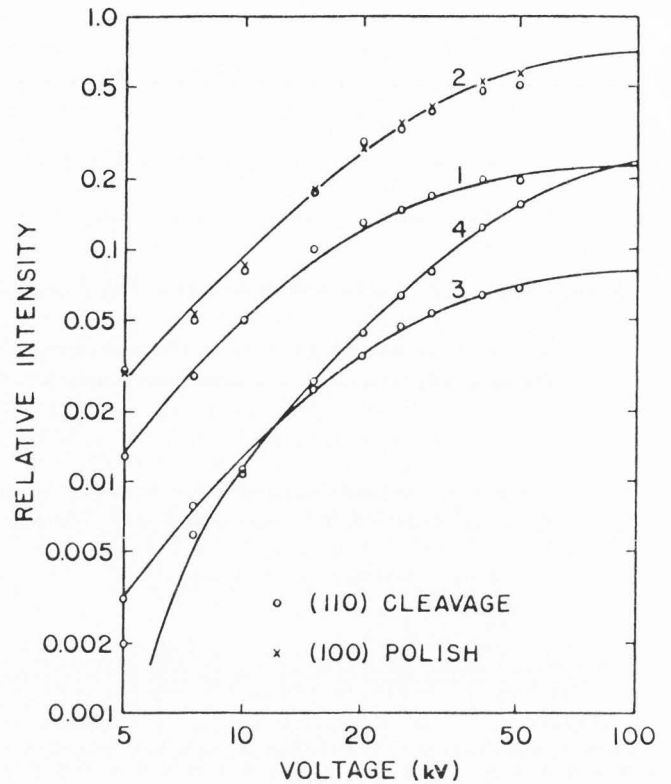


Fig. 12. Comparison of the theoretical and experimental results for the voltage dependence of cathodoluminescence. The correct matching of experimental and theoretical curves provides values of the diffusion L , the reduced surface recombination velocity S and the width of the "dead layer" d (from Wittry and Kyser, 1967).

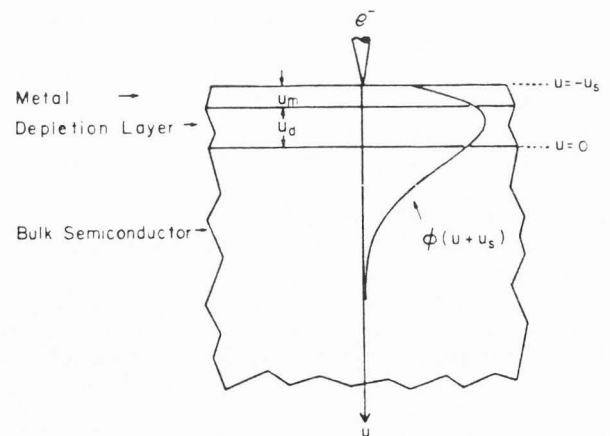


Fig. 13. Model for the calculation of electron beam induced currents (from Wu and Wittry, 1978).

Gaussian Models for Energy Distribution of Excitation

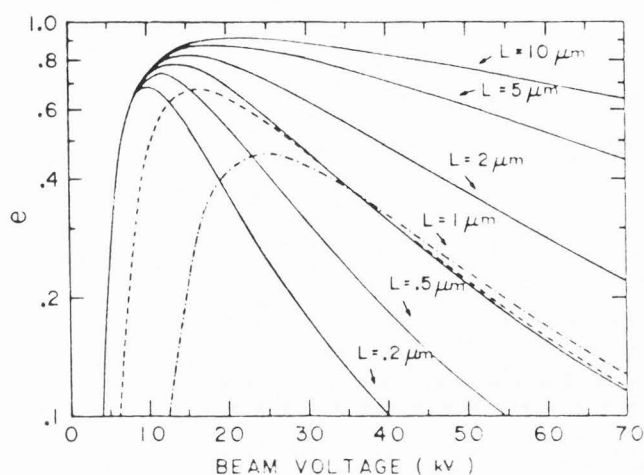


Fig. 14. Theoretical variation of electron beam induced current collection efficiency e at a Schottky barrier on GaAs as a function of beam voltage for various values of diffusion length L . The solid curves were calculated for a gold metal layer 250 Å thick and a depletion layer 0.2 μm thick. Dash and dash-dot curves were calculated for a metal layer of 500 and 1500 Å thick respectively with a depletion layer 0.2 μm (from Wu and Wittry, 1978).

SUMMARY

The Gaussian model for distribution of excitation with depth and the principle of scaling has been found to be useful for many experiments involving electron beam excitation. Up to now, relatively simple models have provided theories adequate for interpreting experimental results in specific cases where parameters in the Gaussian model were determined from experimental data or from transport equations or Monte Carlo calculations. A generalization of the parameters in a Gaussian model as described in a paper by Brown in this publication should provide even more accuracy and easier application of Gaussian models to experiments involving electron beam excitation of solids.

REFERENCES

- Andersen CA. (1966). Electron probe analysis of thin layers and small particles with emphasis on light element determinations, in: *The Electron Microprobe*, T.D. McKinley, K.F.J. Heinrich, D.B. Wittry (eds.), John Wiley & Sons, New York, 58-74.
- Andersen CA, Wittry DB. (1968). An evaluation of absorption correction functions in electron probe microanalysis. *Brit. J. Appl. Phys. (J. Phys. D)*, **1**, 529-539.
- Bishop HE. (1965). A Monte Carlo calculation on the scattering of electrons in copper, *Proc. Phys. Soc.* **85**, 855-866.
- Bishop HE. (1967). Electron scattering in thick targets, *Brit. J. Appl. Phys.* **18**, 703-15.
- Brown DB, Wittry DB and Kyser DF. (1969). Prediction of x-ray production and electron scattering in electron probe analysis using a transport equation. *J. Appl. Phys.* **40**, 1627-1636.

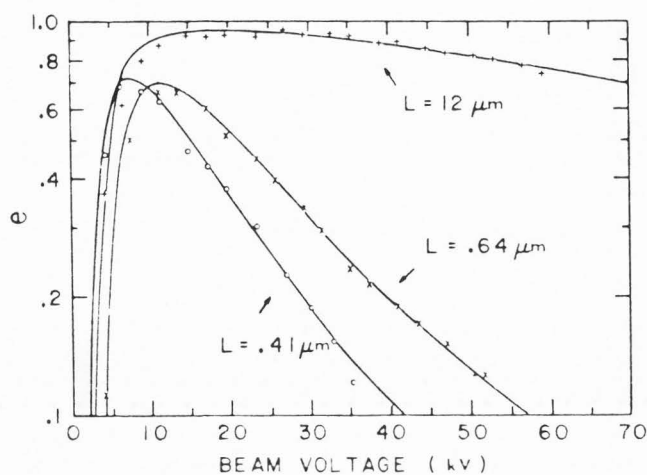


Fig. 15. Comparison of experimental and theoretical results for electron beam induced currents at Schottky barriers in GaAs. The correct matching of experimental and theoretical curves provides values for the metal layer thickness, and the diffusion length L (from Wu and Wittry, 1978).

Brown JD, Parobek L. (1978). The atomic number corrections in electron microprobe analysis at low energies, *X-ray Spect.* **7**, 26-30, errata, *ibid* **8**, v.

Brown JD, Robinson WH. (1979). Quantitative analysis by $\phi(\rho z)$ curves, in: *Microbeam Analysis—1979*, D.W. Newbury (ed.), San Francisco Press, 238-240.

Castaing R, Descamps J. (1953). On the distribution of x-radiation with depth in an anticathode, *C.R. Acad. Sci.* **237**, 1220-2.

Castaing R, Henoc J. (1966). Répartition en profondeur du rayonnement caractéristique, in: *X-ray Optics and Microanalysis*, R. Castaing, P. Deschamps, J. Philibert (eds.), Hermann, Paris, France, 120-126.

Duncumb P, Melford D. (1966). Quantitative applications of ultra-soft x-ray microanalysis in metallurgical problems, in: *X-ray Optics and X-ray Microanalysis*, R. Castaing, P. Deschamps, J. Philibert (eds.), Hermann, Paris, France, 240-252.

Everhart TE, Hoff PH. (1971). Determination of kilovolt electron energy dissipation vs. penetration distance in solid materials. *J. Appl. Phys.* **42**, 5837-5846.

Green M. (1963). The target absorption correction in microanalysis, in: *X-ray Optics and X-ray Microanalysis*, H.H. Pattee, V.E. Cosslett, A. Engström (eds.), Academic Press, New York, 361-377.

Kyser DF. (1972). Experimental determination of mass absorption coefficients for soft x-rays, in: *X-ray Optics and Microanalysis*, G. Shinoda, K. Kohra, T. Ichinokawa (eds.), U. of Tokyo Press, 147-156.

Kyser DF, MacQueen HR. (1972). New absorption correction for soft x-rays in quantitative electron probe micro-

analysis, Proc. Seventh Annual Conference on Electron Probe Microanalysis Society (available from San Francisco Press), 10A-10E.

Kyser DF, Wittry DB. (1967). Spatial distribution of excess carriers in electron beam excited semiconductors, Proc. IEEE **55**, 733-734.

Packwood RH, Brown JD. (1980). Concerning x-ray production and quantitative analysis, in: Microbeam Analysis—1980, D.B. Wittry (ed.), San Francisco Press, 45-48.

Packwood RH, Brown JD. (1981). A Gaussian expression to describe $\phi(\rho z)$ curves for quantitative electron probe microanalysis, X-ray Spectrometry **10**, 138-146.

Philibert J. (1963). A method for calculating the absorption correction in electron probe microanalysis, in: X-ray Optics and X-ray Microanalysis, H.H. Pattee, V.E. Cosslett, A. Engström (eds.), Academic Press, New York, 379-92.

Rao-Sahib TS, Wittry DB. (1969). Measurement of diffusion lengths in p-type gallium arsenide by electron beam excitation. J. Appl. Phys. **40**, 3745-3750.

Wittry DB. (1958). Resolution of electron probe microanalyzers. J. Appl. Phys. **29**, 1543-1548.

Wittry DB, Kyser DF. (1967). Measurement of diffusion lengths in direct gap semiconductors by electron-beam excitation. J. Appl. Phys. **38**, 375-382.

Wu CJ, Wittry DB. (1978). Investigation of minority-carrier diffusion lengths by electron bombardment of Schottky barriers. J. Appl. Phys. **49**, 2827-2836.